2013 IEEE International Conference on Robotics and Automation (ICRA)
Karlsruhe, Germany, May 6-10, 2013

A Compliant Hand Based on a Novel Pneumatic Actuator

Raphael Deimel[1] Oliver Brock[1]

***Abstract*— The RBO Hand is a novel, highly compliant robotic hand. It exhibits robust grasping performance, is easy to build and prototype, and very cheap to produce. One of the primary design motivations is the extensive leverage of compliance to achieve robust shape matching between the hand and the grasped object. This effect results in robust grasping performance under sensing, model, and actuation uncertainty. We show the feasibility of our approach to constructing robotic hands in extensive grasping experiments on objects with varying properties, included water bottles, eye glasses, and sheets of fabric. The RBO hand is based on a novel pneumatic actuator, called PneuFlex, which exhibits desirable properties for robotic fingers.**

I. Introduction

We present a novel robotic hand that embraces the use of passive compliance as a major design principle. Compliance enables the hand to orient its surfaces to that of an object in response to contact forces; we call this effect *shape match*. A good shape match increases the contact surface between hand and object without the need for explicit sensing and control. It also increases the robustness to uncertainties in hand position, finger control, and the model of the environment. In addition, a hand passively compliant in all directions can make contact with the environment without getting damaged. This enables the RBO hand to use the environment as a guide during grasping motion, further increasing the robustness of the grasp. Compliance therefore represents a major factor in improving grasp success under uncertainty—a key objective in the design of robotic hands. Furthermore, passive compliance makes hands safe for use around humans.

The RBO hand (see Figure 1, RBO stands for Robotics and Biology Laboratory) uses a novel pneumatic actuator design in its fingers. These actuators are built entirely out of flexible materials and are thus inherently compliant. The air used to actuate is compressible too, so compliance is retained during actuation. The palm of the hand is also made from flexible materials, exhibiting substantial passive compliance.

The manufacturing process for the RBO hand is simple and fast. One can successfully build a hand on the first attempt within a couple of days. Material costs for the hand shown in Figure 1 are approximately US$25. The ability to have fast manufacturing turn-around allows us to quickly explore the design space, driving effective innovation in hand design. The low cost makes capable robotic hands affordable to more researchers.

We gratefully acknowledge support from the Alexander von Humboldt foundation, funded by the Federal Ministry of Education and Research (BMBF), and from the First-MM project (European Commission,FP7-ICT-248258). We also thank Ivo Boblan for his support and advice.

[1]Robotics and Biology Laboratory, Technische Unverisität Berlin

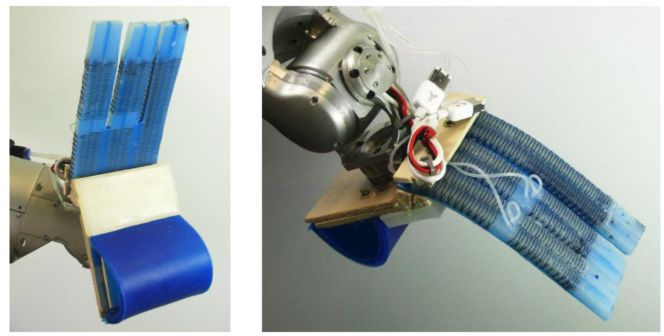

Fig. 1: The RBO Hand is a three-fingered hand with a palm made from silicone pads (blue and white). The parts are mounted onto a plate connected to the wrist of a robotic arm. The fingers are made of reinforced silicone rubber and are pneumatically actuated.

In the remainder of this paper, we first describe the novel pneumatic actuator in Section III and the manufacturing process in Section IV. Section V then describes the design of the RBO hand. We evaluate the performance of the RBO hand in Section VI with two different types of grasps in 1,240 grasping trials on ten different objects, ranging from filled water bottles to sheets of paper. We emphasize that the RBO hand described here is a first prototype based on a new design objective, a novel actuator, and a novel manufacturing process. In this first prototype, we focused on the realization of power grasps. However, we believe the general concept extends to inherently compliant, soft hands capable of performing power grasps, precision grasps, and dexterous in-hand manipulation.

II. Related Work

The use of shape matching and compliance can be found in a number of recently published mechanisms. This section analyzes implementations of related compliant grippers and relates them to the presented hand.

SDM Hand: The design of the SDM Hand also embraces compliance as a central design objective [1]. Even though it is a simple mechanism, great care was taken to design its compliance. Mechanical coupling through tendons balances grasping forces between all fingers. The elastomer joints are compliant, improving the hand's capability to match shapes of objects. In contrast to the RBO hand, the SDM Hand is based on rigid finger links and uses an opposing finger configuration. In a recent extension to the design [2], the fingertips of the SDM hand were patterned with small ridges, enabling picking up a coin from a flat surface.

978-1-4673-5642-8/13/$31.00 ©2013 IEEE

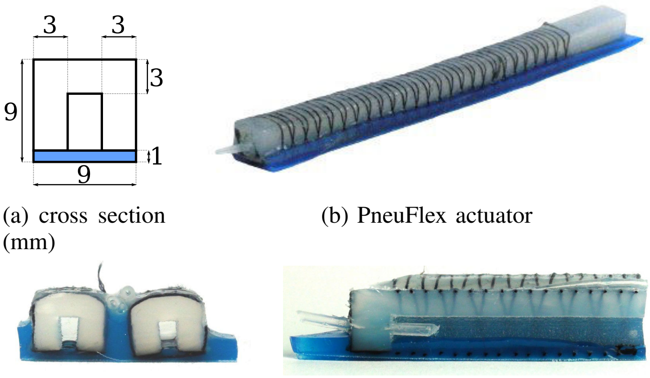

(a) cross section (mm) (b) PneuFlex actuator

(c) finger cross section (d) longitudinal cut

Fig. 2: The PneuFlex actuator: The passive layer (blue, bottom) and the active layer (transparent, top) form a silicone tube filled with air. The tube is reinforced with woven fabric in the passive layer (thin white line), and a helically wound thread (black) around the active layer. A silicone tube is inserted at one end to connect the air chamber.

Pneumatic Anthropomorphic Hand: This hand uses pneumatically inflatable chambers to actuate rigid links [3]. The compliance of the actuator itself is similar to the one used in the RBO Hand. The use of rigid finger links and hinge joints, however, reduces its ability to match the shape of an object during grasping. The designers did not investigate the effects of compliance in subsequent research [4].

Starfish Gripper: The Starfish Gripper [5] is made entirely out of silicone. Its simple symmetric design allows each flexible finger to comply to the object's shapes. The Starfish Gripper is based on PneuNet actuators, which are based on the same principle as the actuators of the RBO Hand, but at ca. 5-10 times lower air pressures, resulting in much weaker actuation and grasping forces.

Positive Pressure Gripper: The Positive Pressure Gripper [6] consists of a rubber balloon filled with ground coffee, whose phase can be altered from fluid to solid by evacuating it. When fluid, the gripper can match the shape of relatively small or thin objects, such as coins, screws and pens. The gripper is limited to a single synergy, as it needs a supporting surface to grasp against, i.e. it cannot grasp free-standing objects like the RBO Hand is able to.

Awiwi Hand: The Awiwi hand achieves compliance through a tendon-driven, antagonistic actuation system [7]. It is probably the most capable anthropomorphic robot hand built to this day. However, it is mechanically very complex, expensive, and requires sophisticated control. From a design perspective, we pursue an opposing philosophy.

III. Actuator Design

Our new continuum actuator is inspired by the PneuNet actuator [5] and is based on the unimorph actuator principle, perhaps best known from bimetal thermostats. The actuator is shown in Figure 2. Two sheets of different materials form a sandwich. A physical process causes them to elongate differently, with the so-called *passive layer* elongating less than the *active layer*. This causes the actuator to bend, as shown in Figure 3.

This principle is implemented in our actuator design with rubber (silicone) as the main passive and active layer material and air pressure to elongate it. The basic shape of the actuator resembles a square tube with closed ends. The chamber can be inflated and deflated with an inserted supply tube. Without any additional reinforcements, such an actuator would expand like a balloon in every direction.

The key to directed motion is anisotropic elasticity. By making the rubber only elastic in one direction, the deformation is fully translated into directed elongation. The PneuNet [5] design implements anisotropy by varying the thickness of the walls. This approach is easy to manufacture, but it is limited by the small ratios in elasticity that can be achieved. To overcome this limitation, our novel PneuFlex actuator embeds polymer fibers to reinforce the rubber substrate. Polymers, such as polyethylene terephtalate (PET), are three to four orders of magnitude less elastic than silicone. We use polymer fibers for two distinct tasks.

In the *passive layer*, embedded fibers enable bending without significant elongation. The *reinforcement helix* along the entire actuator creates anisotropic elasticity in the active layer. These design changes result in significantly improved performance, both in terms of attainable curvature and actuator linearity as the measurements show in Figure 4.

Passive Layer Reinforcement: We embed a woven sheet of polymer fabric in the passive layer. The passive layer remains flexible for bending but effectively does not elongate any more. In our design explorations, this solution proved superior to embedding other materials, such as paper and felt, as the silicone was able to permeate the woven sheet.

Reinforcement Helix: A thread (sewing thread) is wound around the actuator to constrain the expansion of the actuator during actuation and to reduce mechanical strain. The effect is increased bending of the actuator under constant pressure.

The ideal form of reinforcement would be a series of separate rings along the actuator, to give a maximally anisotropic elasticity [8]. We used a helix instead, as using a single thread is easier to manufacture and avoiding knots removes points of failure. As a trade-off, local forces are introduced in the rubber, and therefore stretch is not perfectly uniform. We found the double helix with opposite winding directions to be a good compromise.

The reinforcement helix suppresses ballooning, an undesirable failure, leading to the thinnest part the rubber wall blowing up like a small balloon. The silicone there is stretched well into its plastic range, wearing out quickly.

When the actuator is inflated, the helix forces the actuator to deform into a cylindrical tube. An initially circular cross section avoids this deformation, but for simplicity of manufacturing, we chose a square shape for the actuators. If desired, an initially flat tube can even be used to alter actuator behavior between low and high pressures.

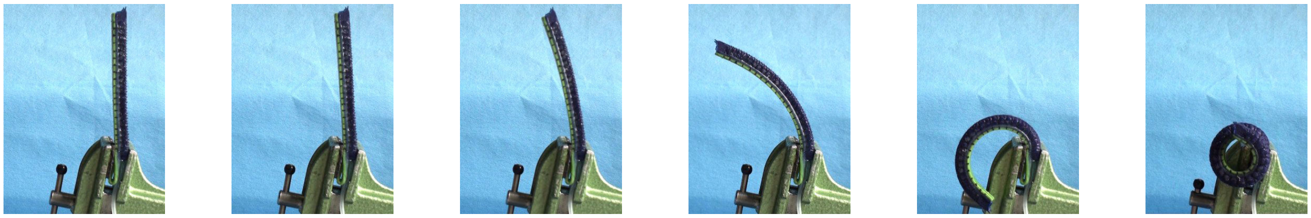

(a) 0 kPA (b) 10 kPa (c) 30 kPa (d) 50 kPa (e) 100 kPa (f) 150 kPa

Fig. 3: PneuFlex actuator bending at different pressures: the curvature is uniform along the actuator and absolute length does not change significantly ($< 5\%$). The diameter of the actuator is kept constant by the reinforcement helix. The shown actuator is made of silicone EcoFlex 50 and 4mm felt in passive layer.

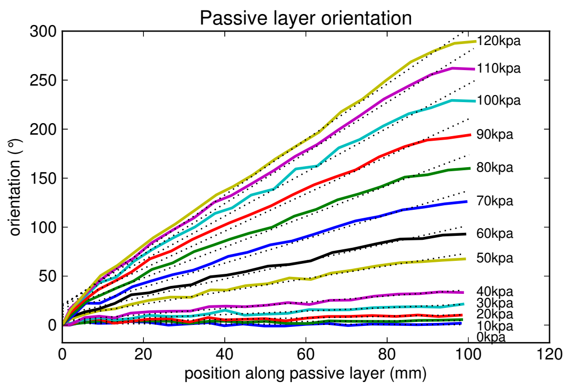

(a) Orientation of passive layer along actuator

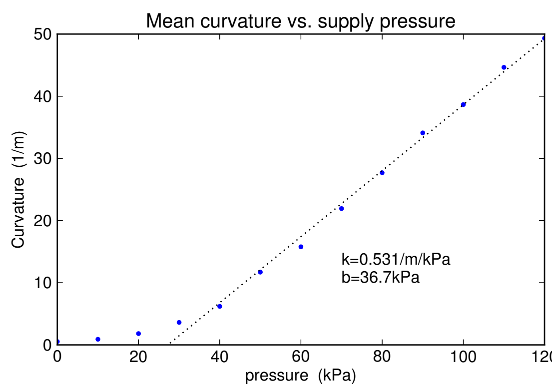

(b) Actuator response and linearized model.

Fig. 4: Measurements with unloaded actuator in Figure 3

A. Applicability

There are no rigid moving parts in the actuator, which makes it very robust against blunt collision. The actuator can safely collide with other objects, such as tabletop surfaces or walls, without applying harmful levels of force on the environment or itself. Compliance and low inertia make the robot safe for human interaction. The actuator works reliably in dusty, wet, and outdoor environments, which usually are problematic to mechatronic actuators [9]. It is also easy to sterilize, and cheap enough for one-time use. This makes the actuator interesting for medical and biotechnological applications. All of these properties make the PneuFlex actuator very attractive in the context of robotics. It has the disadvantage, however, of being susceptible to punctures by sharp objects.

B. Strength

The strength of the actuator is affected by its shape, the stiffness of the material, and the employed pressure. In the specific implementation described here, one finger of the RBO hand can produce about 1.5 N force at the finger tip. This was sufficient for initial experiments, as we managed to grasp objects of up to 0.5 kg (see Table II). If necessary, the strength of the actuator can be increased by several means. The attainable forces scale with the square of the diameter of the actuator, so using a thicker actuator would be one option. Though, this comes with the trade off of reducing the attainable curvature given the same air pressure. One can also switch to different materials and production techniques. We imagine that a hydraulic version of the actuator made of butyl rubbers and steel fibers would be able to create forces sufficient for most applications. Actuator strength therefore is not an inherent limitation for the PneuFlex design.

C. Fatigue

Rubber is subject to wear and fatigue, and "remembers" episodes of excessive stretch (Mullins effect [10], for a analysis of mechanical fatigue in silicones, see [11]). To keep the actuator usable for a long time, we need to keep the maximal stretch as low as possible. Thanks to the reinforcement helix, the curvature c of the passive layer is related to the highest mechanical stretch λ in the active layer with $c \approx \frac{(\lambda-1)}{d}$, where d is the height of the actuator. This relation also shows that bending is limited by the stretchability of the active layer. To minimize fatigue, the actuators used in the RBO Hand are designed to stay below $\lambda \approx 2$, which is 2-5 times lower than the maximum stretch of the material. We successfully performed more than 2000 load cycles on six specimen during experimentation without failures.

IV. Manufacturing Process

The manufacturing process of the PneuFlex actuator is additive and uses printed molds. This makes the customization and combination of actuator shapes simple and supports the implementation of complicated deformations. Together with

Fig. 5: Two-part mold, casts, and complete active layer with reinforcement helix

low material costs and fast manufacturing process, it enables rapid prototyping of robotic hands.

1) Active Layer casting: The active layer is cast using a closed two-part mold shown in Figure 5 to ensure a reproducible form. The mold is 3D-printed using epoxy-resin impregnated plaster. Additionally, the silicone mold features small ridges to imprint groves along the edge of the silicone to hold the thread of the reinforcement helix in place during manufacture. Casting is done by evacuating the mold in a vacuum chamber (to about 5kPa) and filling in the silicone by gravitational flow. We can report this simple technique to work for silicones of up to 30,000mPas viscosity and cross sections as small as 3mm.

2) Reinforcement Helix winding: We use sewing thread (size 50) made of of polyethylene terephtalate (PET) to wind the reinforcement helix. This material is very flexible, yet can transmit high tensile forces at low strain. To evenly distribute strain in the silicone between the turns, the helix has a low pitch (4mm per winding). We use two helices wound in opposing directions to neutralize torsional force. The thread crosses itself only on the sides of the actuator. Such crossing patterns were previously investigated [12]; we chose it to increase torsional rigidity while reducing interference with the bending motion.

3) Passive Layer casting: As silicone rubbers are difficult to bond to other materials, creating compound structures difficult. We reinforced the passive layer with a porous fabric embedded into and permeated by silicone. This gives good bonding and enables transmission of significant forces. Table I shows results from experiments with different reinforcement materials. For the RBO Hand, silkscreen was used, and the fibers were aligned with long side of the actuator. The passive layer is cast by placing the fabric on a horizontal tray made of polypropylene, covering it 2-3mm high with silicone, and degassing it in a vacuum chamber.

4) Assembly: Before the silicone sets, the active layer is placed on top of the passive layer, bonding them together to form the final actuator. In the final step, the embedded air chambers are connected via silicone tubes (0.5mm inner/1.5mm outer diameter), which are inserted into the silicone using a 2mm canula and sealed using pasty silicone adhesive.

Material	Strain behavior	Bonding	common failure
PET silkscreen 43 tpi threads 80 μm	non isotropic negligible along fibers high at 45° angle	excellent	single fibers loosen
Felt (65% wool, 35% PET) 2 mm	moderate isotropic low strength	good	rips
PET woven tablecloth thickness 200 μm	non isotropic, low along fibers high at 45° angle	good	single threads loosen
Felt (65% wool, 35% PET) 4 mm	low, isotropic inflexible	good	rips
paper 80 g/m^2	negligible isotropic	poor	delaminates, breaks
Polycarbonate foil 0.5 mm	negligible isotropic	poor	delaminates
Polyethylene Polypropylene	negligible isotropic	very poor	delaminates

TABLE I: Comparison of tested reinforcement materials, ordered by suitability for the passive layer

V. The RBO Hand

The RBO Hand features several properties that usually are considered undesirable in robotic manipulators. Its behavior is nonlinear, positions and forces are not independently controllable, and faithful mechanical models are difficult to come by. To make things worse, material properties change significantly over time and generally show a high variance between specimen due to tolerances in production and material [11].

The design of the hand attempts to use the characteristics of the actuators to our advantage. By choosing a clever morphology, we do not need to independently control all possible degrees of freedom. A highly compliant hand already features a lot of internal mechanical feedback (sometimes called morphological computation) that makes grasping much more robust against variations in pre-grasp position, environment, and object shape. As a consequence, misperceptions of geometry and position are less likely to cause grasp failure.

A. Implementation

In the first prototype of the RBO Hand, we chose to give it 3 fingers, each consisting of two parallel PneuFlex actuators. Two of the three finger's actuators were split to be able to independently control flexion along the finger. The palm was split into two sections, a flat pad of very soft silicone (translucent, EcoFlex 30, 10mm thick), and a bent rubber plate (blue tinted, DragonSkin 20, 3mm thick). The latter structure creates a very soft pad to match object shapes well.

The frame of the RBO Hand consists of a simple plate of plywood (80x80x3mm, 3-ply, birch) to mount the silicone parts to the robotic arm. We found this assembly to be robust, easy to manufacture and quick to adapt during rapid prototyping.

The total length of each finger is 130mm. One finger has two actuators of 95mm length each, with an unactuated tip of 30mm length. In the other two fingers, the air chambers were additionally split up in two segments of 35mm and 45mm length, separated by 10mm. Each finger has a cross section of 9×21mm, and is made of DragonSkin 10 silicone, silkscreen fabric and size 50 PET sewing thread. The fingers are mounted to the metacarpal plate at a 30° angle. Together with the passively compliant palm, the flexible fingers implement a power grasp for cylindrical, spherical, and hyperbolic shapes.

The finger posture can be controlled by two supply tubes, one for the actuators at the distal part of the split fingers, and one for the all other actuators.

B. Control

In the context of this paper, we use open loop control for the RBO Hand. An external reservoir supplies pressurized air and industrial grade solenoid valves attached to the supply tubing control inflation and deflation of the hand. The control system was used to play back scripted sequences of valve actuations.

VI. Experimental Results

The performance of the RBO Hand was tested in two experiments. In the first one, common human artifacts placed on a table were grasped from the side, following the experimental scenario chosen by others [13], [14]. The key feature of this grasp is the compliance of the object as it slides along a surface and therefore we prefer to call it a *sliding grasp*, instead of the name *push grasp* used in other research. In the second experiment, the RBO Hand grasps the object from the top. Also this evaluation scenario has been used previously [6], [1], [14]. In this paper, we refer to this grasp as *surface-constrained grasp*. By choosing these two experimental setups we cover the two most commonly used experimental scenarios for evaluating grasp performance of hands.

A. Experimental Setup

The RBO Hand was mounted on a seven degree-of-freedom robotic arm (Meka Robotics A2) for positioning and execution of the synergy. Control of the hand and arm during grasping was done without sensory feedback.

In each experiment, an object is placed as close as possible to a reference frame origin (see Figure 8a), while keeping its full volume in the $y < 0$ and $x > 0$ half-spaces, touching the $x-z$ and $y-z$ planes. We chose this placement because surfaces are usually much easier to perceive (visually) than for example center of mass or symmetry axes. The hand is then positioned in a fixed configuration relative to the object. Then the arm and hand perform a scripted grasp. To perform the grasp, the actuators are inflated to 210kPa. Following the grasp, the hand is lifted 100mm along the z-axis, holds still for 1s, and lowering the hand again, in small jerking steps, for a total duration of 7s. A grasp is deemed successful if the object followed the hand's motion, did not slip, and only contacted the RBO Hand.

object	**surface** material	**size** mm	**weight** g
water bottle	PET	⌀63 × 215	546
tube	PVC	⌀33 × 178	114
cylinder	cardboard	⌀65 × 175	106
water balloon	late× rubber	125 × 63 × 35	99
tape dispenser	PP/PE	56 × 28 × 77	30
staple remover	metal, PP	57 × 47 × 32	20
sunglasses	glass, metal	125 × 36 × 23	16
marker	PP/PE	⌀17 × 138	14
paper cup	paper	⌀88 × 110	13
tissue	PET fiber	150 × 150 × 0.2	1

TABLE II: Key data of tested objects

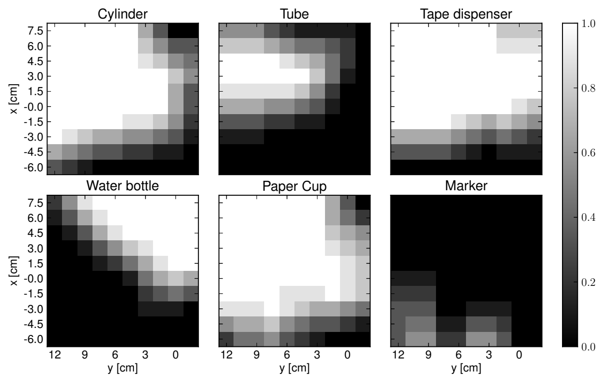

Fig. 7: Sliding grasps success probabiliy under object placement variation

Objects were selected to vary significantly in size, weight, shape, surface texture, and rigidity. We did not include objects that exceeded the inherent weight or size limitations of the hand.

To keep the number of trials to a realistic range, the experiment was restricted to only vary object type and two spatial variables (object's (x, y) position) with an otherwise fixed action sequence and environment (see also [1]). In total, we conducted 1240 trials on ten different objects with two different grasps. Each object position was tried only once, and the success was recorded. The results are filtered with a 3×3 sliding window average, to estimate probabilities of grasp success over the x/y-plane.

We expected the hand to be able to grasp all objects at least at one place, and that generally due to the compliance of the hand, we should find contiguous areas of successful grasps.

B. Sliding Grasp Results

For this experiment, objects were grasped from the side along a horizontal support surface (table, surface: paper) from a fixed pre-grasp position. The hand moves forward, making contact with the object and possibly pushing it along the surface. The fingers are then flexed to cage and contact the object between fingers and palm.

Results in Figure 7 show that the hand can grasp most tested objects in a contiguous range of object placements,

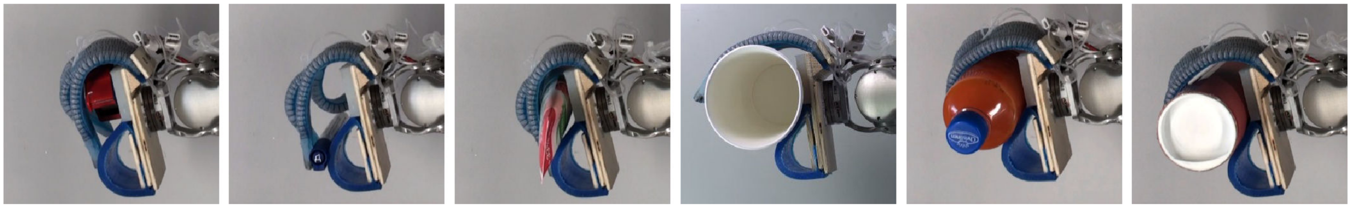

Fig. 6: Examples of successful sliding grasps; objects are shown in Figure 8a

(a) left to right: tape dispenser, marker, tube, paper cup, water bottle, cylinder

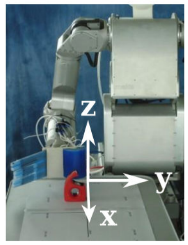

(b) reference frame

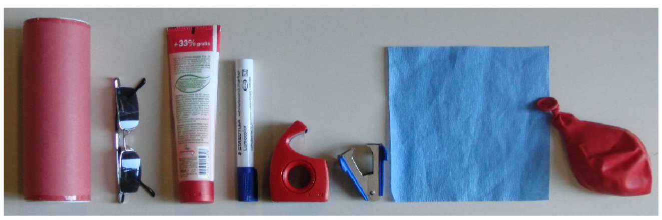

(c) Left to right: cylinder, sun glasses, tube, marker, tape dispenser, staple remover, tissue, water balloon

Fig. 8: Objects used in grasping experiments

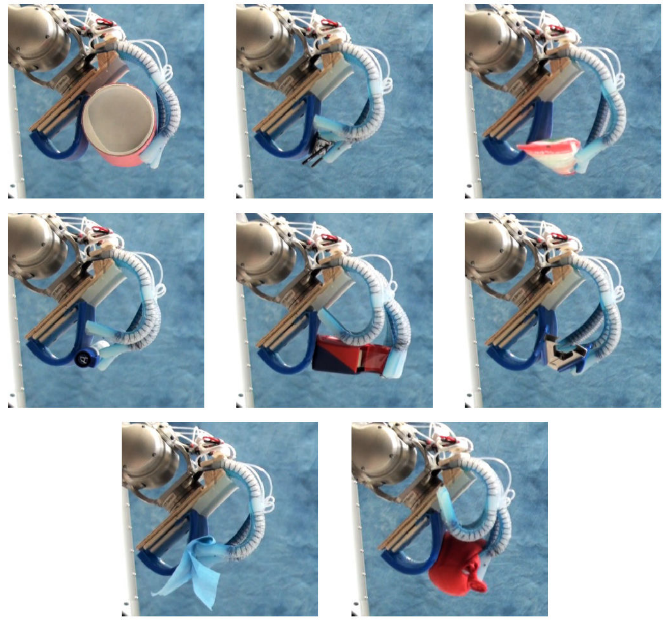

Fig. 10: Examples of a successful surface-constrained grasps; objects are shown in Figure 8c

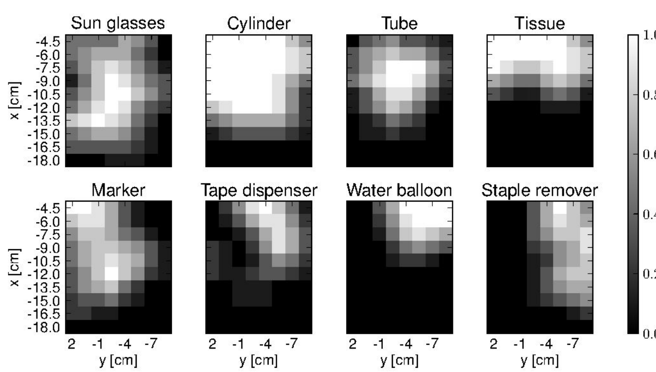

Fig. 11: Surface-constrained grasp success probability under object placement variation

which indicates a tolerance to position uncertainties. Although there are significant differences between the tested objects, a robot capable of distinguishing between them could easily select a reliable action sequence for each. The most difficult object tested was the marker (shown in Figure 8a), whose outer diameter is smaller than the inner diameter of the fully flexed fingers. It escapes the grasps when only caged, and generally falls over when being pushed (shown in Figure 12). Still, the RBO hand managed to grasp the marker in eight positions, which cluster in two regions and correspond to two distinct grasp mechanisms. Exploiting these two displacements necessitates a very precise positioning of the object though.

Examples of other sliding grasping failures are show in Figure 12.

C. Surface-Constrained Grasp Results

The surface-constrained grasp exploits the support surface to guide the grasping motion, leveraging the strengths of a highly compliant hand. The tested objects are shown in Figure 8. For each experiment, the hand is positioned above the object and approaches the table surface from top down, with the palm pitched at 45°. The individual steps are shown in Figure 9. In these experiments, the hand displacements were varied relative to the object.

The results in Figure 11 are similar to those of the first experiment in Figure 7. All objects show a contiguous region in parameter space. This is expected when using compliant mechanisms, as they often exhibit gradual failure modes rather than abrupt changes in performance. The regions of success are comparable to other compliant hands as surveyed in [6]. Even though object properties vary significantly, the regions of success possess large overlaps—an indication that the RBO Hand indeed is able to grasp many objects without

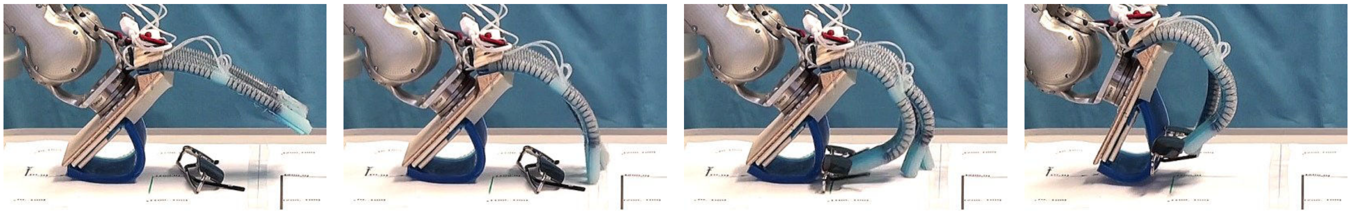

Fig. 9: Surface-constrained grasp: contacting the surface, caging the object, contacting the object, pitch to lift

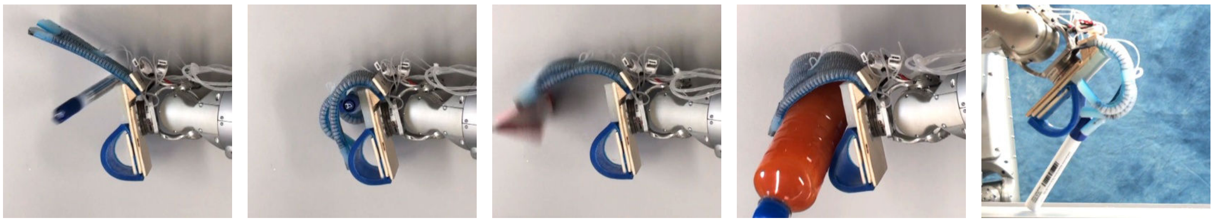

(a) tipping over (b) caging, no contact (c) fingers eject object (d) slipping (e) slipping

Fig. 12: Examples of grasp failures

prior knowledge of their exact shape.

We observed a fuzzy transition between the regions of success and failure with the sunglasses and marker that did not occur with the other objects. This suggests that these objects are difficult to grasp.

VII. Conclusion

We presented the RBO Hand, a highly compliant robotic hand. It is constructed using the novel PneuFlex actuator, a low-cost pneumatic actuator made of silicone rubber and polyester fibers. The goal of the hand design is to take maximum advantage of compliance to achieve robust grasping performance. Our experiments demonstrate that the RBO Hand achieves reliable grasping performance without feedback and only based on very simple control. At the same time, the RBO Hand is easy and cheap to manufacture, putting grasping capabilities into the hands of many roboticists and enabling fast prototyping and development. The hand is also safe for use in human-robot interaction. Its construction makes it suitable for use under a variety of environmental conditions, including wetness, dustiness, high and low temperatures, sterility, among others. We believe that this novel way of constructing hands could lead to simple and competent end-effectors for mobile manipulation.

References

[1] A. M. Dollar and R. D. Howe, "The highly adaptive SDM hand: Design and performance evaluation," *The International Journal of Robotics Research*, vol. 29, no. 5, pp. 585–597, 2010.

[2] R. Ma, L. Odhner, and A. Dollar, "Dexterous manipulation with underactuated fingers: Flip-and-pinch task," in *IEEE International Conference on Robotics and Automation (ICRA)*, 2012, pp. 3551–3552.

[3] S. Schulz, C. Pylatiuk, and G. Bretthauer, "A new ultralight anthropomorphic hand," in *IEEE International Conference on Robotics and Automation, Proceedings ICRA*, vol. 3. IEEE, 2001, pp. 2437–2441 vol.3.

[4] A. Bierbaum, J. Schill, T. Asfour, and R. Dillmann, "Force position control for a pneumatic anthropomorphic hand," in *9th IEEE-RAS International Conference on Humanoid Robots, Humanoids*. IEEE, 2009, pp. 21–27.

[5] F. Ilievski, A. D. Mazzeo, R. F. Shepherd, X. Chen, and G. M. Whitesides, "Soft robotics for chemists," *Angewandte Chemie International Edition*, vol. 50, no. 8, pp. 1890–1895, 2011.

[6] J. Amend, E. Brown, N. Rodenberg, H. Jaeger, and H. Lipson, "A positive pressure universal gripper based on the jamming of granular material," *IEEE Transactions on Robotics*, vol. 28, no. 2, pp. 341–350, 2012.

[7] M. Grebenstein, "Approaching human performance: The functionality driven awiwi robot hand," Ph.D. dissertation, ETHZ, 2012.

[8] Joshua Bishop-Moser, Girish Krishnan, Charles Kim, and Sridhar Kota, "Design of soft robotic actuators using fluid-filled fiber-reinforced elastomeric enclosures in parallel combinations," in *IEEE/RSJ International Conference on Intelligent Robots and Systems (IROS)*, 2012.

[9] J. Butterfass, M. Fischer, M. Grebenstein, S. Haidacher, and G. Hirzinger, "Design and experiences with DLR hand II," in *World Automation Congress*, vol. 15, 2004, pp. 105–110.

[10] L. Mullins, "Softening of rubber by deformation," *Rubber Chem. Technol.*, vol. 42, pp. 339–362, 1969.

[11] P. Meier, M. Lang, and S. Oberthür, "Reiterated tension testing of silicone elastomer," *Plastics, Rubber and Composites*, vol. 34, no. 8, pp. 372–377, 2005.

[12] M. Hatanaka, "Design and fabrication of multimaterial flexible mechanisms with embedded components," Dissertation, Stanford University, Stanford, 2005.

[13] M. Dogar and S. Srinivasa, "Push-grasping with dexterous hands: Mechanics and a method," in *IEEE/RSJ International Conference on Intelligent Robots and Systems (IROS)*, 2010, pp. 2123–2130.

[14] M. Kazemi, J.-S. Valois, J. A. Bagnell, and N. Pollard, "Robust object grasping using force compliant motion primitives," in *Proceedings of Robotics: Science and Systems*, Sydney, Australia, 2012.